Available online at www.sciencedirect.com
SCIENCE @ DIRECT®
ELSEVIER
Ocean Engineering 30 (2003) 2297–2309
OCEAN ENGINEERING
www.elsevier.com/locate/oceaneng

Technical Note

Micro-bubble resistance reduction on a model SES catamaran

Robert Latorre [a,*], Aaron Miller [b], Richard Philips [c]

[a] *Naval Architecture and Marine Engineering, University of New Orleans, 911 Engineering Building, New Orleans, LA 70148, USA*
[b] *Orion Marine Technology, LLC, 2650 Lincoln Ave., Hollywood, FL 33020, USA*
[c] *Naval Underwater Warfare Center, Newport, Rhode Island, Building 990/1, Newport, RI 02841, USA*

Received 25 September 2002; received in revised form 12 February 2003; accepted 23 February 2003

Abstract

The concept of micro-bubble ejection is emerging as an attractive method for viscous drag reduction for high speed craft. Most of the drag reduction literature presents results for micro-bubble ejection above/below horizontal surfaces. Nevertheless, modern high-speed hull forms are slender with vertical surfaces. This paper presents results of model tests with micro-bubble ejection to the vertical sides of a high speed model with a non-wetting coating. The coating yielded drag reduction of 4–6% and micro-bubbles with coating reduced overall drag by 4–11%. The local coefficient of friction with micro-bubbles is analyzed and found comparable to vertical flat plate results of Madavan et al. (1984).

Keywords: Surface effect ships; Drag reduction; Micro-bubble drag reduction

1. Introduction

There are several techniques to achieve drag reduction on marine vehicles. Documented drag reduction techniques include electrolysis induced micro-bubbles on an axisymetric body (McCormick and Bhattacharyya, 1973), bottom air film (Latorre, 1993, 1997) as well as mirco-bubbles ejected into the boundary layer (Merkle and Deutsch, 1992). The survey of Latorre and Bablenko (1998) showed the reduction in the local skin friction is sensitive to the bubble orientation on the the surface.

* Corresponding author. Tel.: +1-504-280-7180; fax: +1-504-280-5542.
E-mail address: rlatorre@uno.edu (R. Latorre).

0029-8018/$ - see front matter © 2003 Elsevier Ltd. All rights reserved.
doi:10.1016/S0029-8018(03)00079-9

Nomenclature

A_a	aft ejector screen area
A_f	forward ejector screen area
B	beam overall
Cf	coefficient of skin friction resistance
Cf'	coefficient of skin friction resistance with microbubble system
C_V	gas flow ratio
d	diameter
d_b	bubble diameter
d_p	screen pore hole diameter
F_∇	Volumetric Froude Number
g	acceleration of gravity
h_a	aft ejector screen height
h_f	forward ejector height
L	length overall
LCG	longitudinal center of gravity
L_t	tow point attachment position
Q_a	micro-bubble gas flow
Q_w	boundary layer flow
R_f	frictional resistance
R_P	pressure resistance with micro-bubbles
R_{Po}	pressure resistance without micro-bubbles
R_N	Reynolds number
R_T	total resistance with micro-bubbles
R_{To}	total Resistance without micro-bubbles
S	hull wetted surface, plate area m^2
S_b	bubble coating wetted surface
SES	Surface Effect Ship
T	Draft
V	speed, m/s
W	vessel weight
w_a	width of aft ejector screen
w_f	width of forward ejector screen
x	length of surface
x_a	aft screen location from transom
x_f	forward screen location from transom
y_a	aft screen location from lower hull edge
y_f	forward screen location from from lower hull edge
α	Cf'/Cf reduction ratio of skin friction with microbubbles
β	ratio of bubble coated surface to wetted surface
δ	boundary layer thickness

δ'	boundary layer equivalent thickness
$\delta*$	displacement boundary layer thickness
ΔRt	percent change in total model resistance
ΔR_c	percent change in total resistance due to coating
ΔR_b	percent change in total resistance due to micro-bubbles
∇	ship's displaced volume m^3
ρ	density of water
ν	kinematic viscosity of water

The mechanism of micro-bubble drag reduction has not been fully investigated. It appears the micro-bubbles increase the effective viscosity of the air–fluid mixture with a corresponding reduction in the Reynolds stress and a change in the pressure gradient and near wall velocity profile. Micro-bubbles were found to reduce the high frequency component of flush mounted wall sensors (Madavan et al., 1985). Detailed flat plate laser Doppler velocimeter measurements by Kato et al. (1999) showed that when the turbulent boundary layer is filled with bubbles the velocity is decreased near the wall, with a corresponding decrease in the velocity gradient at the wall. The largest reduction was found in the case of bubbles ejected under the bottom surface. However, Fukuda et al's (2000) model tanker experiment showed that bottom air film escapes around the hull sides without the use of longitudinal air guards set at the bilge. For tankers and barges with moderate length to beam L/B hulls, the bottom air covers a large percentage of the wetted surface.

In contrast, high-speed multi-hull ships utilize large L/B slender hulls with long vertical hull sides. Fortunately, vertical plate tests with micro-bubble ejected in the wall boundary layer were completed (Madavan et al., 1984). These tests resulted in a 10–30% reduction in the local coefficient of skin friction C_f. As a contribution to developing a high-speed micro-bubble drag reduction (MBDR) system for the high-speed craft, this paper presents the comparative results from a series of model SES catamaran tests with/without micro-bubbles on the vertical hull sides. The 2.31 m SES catamaran model hull sides were fitted with forward and aft underwater gas generator screens and the model resistance measured with/without the micro-bubble injection during each resistance test run. Additional tests were run with the model coated with a self-polishing, non-wetting coating A with/without micro-bubble ejection (Latorre et al., 2002a; 2002b).

Analysis of the test results showed the micro-bubble ejection with a non-wetting achieved a 10% overall drag reduction corresponding to a 10–15% reduction in the local skin friction.

2. 2.3 m SES catamaran model

For this investigation a 2.3 m model of a 28 m catamaran (1:12 scale) Surface Effect Ship (SES) ferry was used. Fig. 1 shows the 2.3 m SES catamaran model

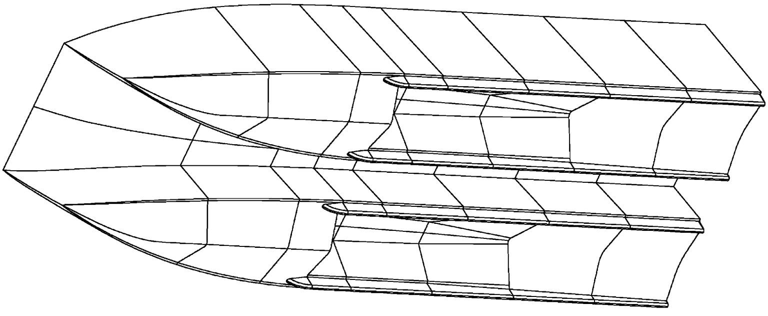

Fig. 1. Bottom view of the SES catamaran used in tests.

with the air cushion cavity in each demi-hull. The particulars of the catamaran model are summarized in Table 1. Resistance tests with the smooth gel-coat model bottom were taken as baseline condition. A single tow post was used—positioned 0.333L, length of the model from the bow. The tow point shaft is mounted in a roller cage which allows vertical heave motion. This assembly was fastened to the model by an aluminum plate using a mount fixture. A turntable with a vertical rotation axis allows 360 degree yaw freedom. A universal joint allowed roll and pitch motion. Torsional moments on the 23 kg load-cell was minimized by a built in parallelogram box. The reaction of tow post weight was eliminated through use of a counterweight.

In addition to resistance, the model sinkage and trim were measured by fore and aft potentiometers. The catamaran wetted surface, *S*, was estimated using sinkage, trim, and model photographs. The towing tank data was recorded through a laptop computer utilizing LabView software (Phillips et al., 2001).

Table 1
Particulars of 2.3 m model catamaran used for MBDR system development

Item	Symbol units	2.3 m catamaran model
Length	*L*, m	2.31
Beam	*B*, m	0.75
Draft	*T*, m	0.015
Displacement	*W*, kg	38.1 kg
Center of gravity	*LCG*, %L	60, 62, 69
Tow position	L_t, %L	33
Wetted surface	*S*, m^2	0.24–0.38
SES blower motor	HP	5
MBDR system		
Gas generator		Nitrogen Bottles
Flow	Q_a, m^3/min	1.13
Ejectors	–	Table 3
Non-wetting coating	–	SuperSpeed SP 52

Table 2
Model MBDR system details

MBDR system	Symbol, units	2.3 m model catamaran
Gas supply	–	Nitrogen gas bottle
Gas flow	Qa, m^3/min.	1.13
Bubble diameter	d_b, cm	20 micron
Ejector no. total	–	2 per demi-hull side × 4=8
Type	–	Screen
Hole	d_p, cm	0.0025
Hole/plate area	−, %	10%
Forward ejector		
Edge from transom	x_f, m	1.03
Edge from bottom	y_f, cm	1.5
Height	h_f, cm	0.95
Width	w_f, cm	4.45
Area	A_f, cm^2	4.23
Aft ejector		
Edge from transom	x_a, m	0.57
Edge from bottom	y_a, cm	1.5
Height	h_a, cm	0.95
Width	w_a, cm	4.45
Area	A_a, cm^2	4.23
Coating		
Superspeed SP52	–	Self polishing
Test area/wetted area	–	0.38–0.68

3. Micro-bubbled drag reduction (MBDR) system

The Micro-Bubble Drag Reduction (MBDR) System consisted of eight hull-side screen mesh injectors. The MBDR system injector details are summarized in Table 2. They were connected to the pressurized nitrogen bottle gas supply by 1.27 cm diameter nylon braid lines. A brass manifold insured equal flow in each of the eight

Table 3
Model test matrix

Item	V_m, (m/s) no coating W/O micro-bubbles	V_m, (m/s) coating A W/O micro-bubbles	V_m, (m/s) coating A W/micro-bubbles	S (m^2)	Ratio β coating A to wetted surface
Temp °C	6	6	6		
Test 1	5.7	5.7	5.7	0.381	0.380
2	6.6	6.6	6.6	0.334	0.433
3	7.5	7.5	7.5	0.297	0.488
4	8.5	8.5	8.5	0.260	0.557
5	9.5	9.5	9.5	0.232	0.624
6	10.4	10.4	10.4	0.214	0.678

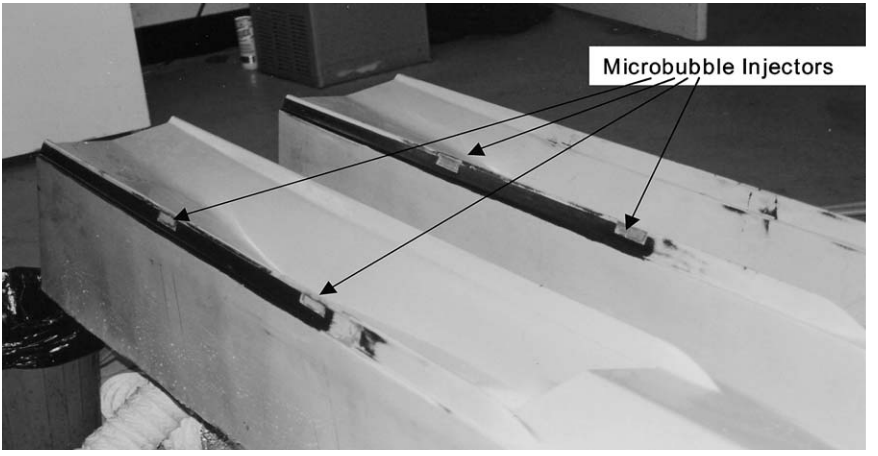

Fig. 2. SES Catamaran model with MBDR system and non-wetting coating A.

ejector sites. Fig. 2 shows four of the ejectors fitted in the vertical sides of the SES catamaran model. To insure micro-bubble coverage, each hull side has two (fore and aft) ejectors.

4. Model tests at Langley sea water towing tank

The catamaran model tests were conducted in the 878 × 7.3 × 3.65 m deep NASA/Langley seawater-towing tank, located in Hampton, Virginia. The tests were organized following Yun and Bliault (1999). An electric fan driven by a variable speed 208 V 3 phase AC motor supplied the cushion air. Fig. 3 shows the catamaran model during a 8.54 m/s run (F_∇ = 4.74).

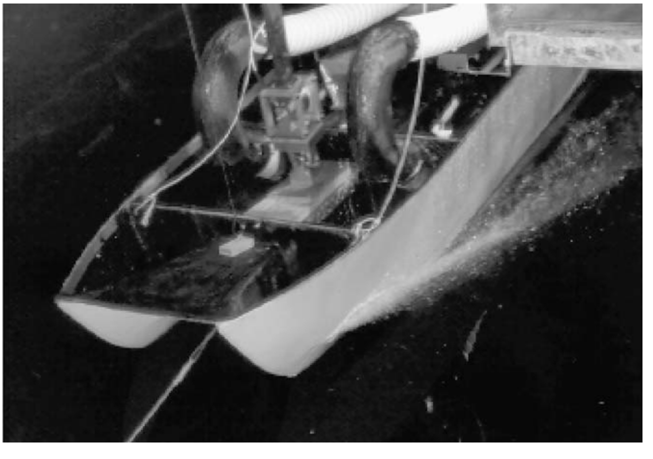

Fig. 3. Catamaran model test, V = 8.56 m/s (F_V = 4.74).

Table 4
Results of the 2.3 SES catamaran tests

Test no.	Speed V_m, m/s	Volumetric Froude no. F_v	ΔR_c Change coating A percent	Total $\Delta R_c + \Delta R_b$ percent
1	5.7	3.16	2.03	1.62
2	6.6	3.68	1.43	3.57
3	8.5	4.72	4.00	5.14
4	9.5	5.26	6.87	11.60
5	10.4	5.78	6.25	8.00

The model test matrix is summarized in Table 4. A second set of tests were made to obtain data on the micro-bubble drag with a self-polishing marine bottom paint. For ease in making comparisons, the self-polishing coating was applied in the same area covered by the micro-bubbles (Fig. 2).

At the start of each run, the SES fan rpm was set and the zeros for each data channel were recorded. When the model reached steady state speed, data for the case of no micro-bubbles was recorded. At this condition the micro-bubble system was switched on for 15 s and turned off for the duration of the run. A typical data record is shown in Fig. 4. The gas flow rate was $Q_a = 1.13\ \mathrm{m}^3/\mathrm{min}$.

The model test speeds, wetted surface, S, and micro-bubble coating ratio, β, are summarized in Table 3. The no-coating baseline tests were completed and then the model was retested with coating A.

The model test results are plotted in the form of R_t/W versus the volumetric displacement Froude number, F_∇ in Fig. 5. The data points represent the average of two to three test runs. The general reduction in total drag ΔR_t = 6–11% with micro-bubbles and coating A, estimated by:

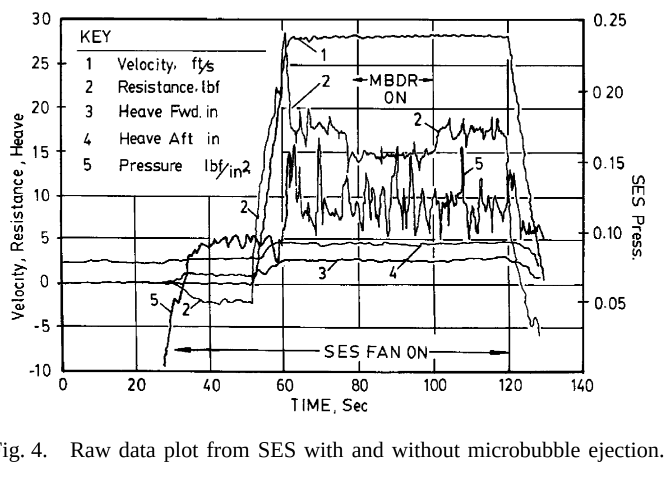

Fig. 4. Raw data plot from SES with and without microbubble ejection.

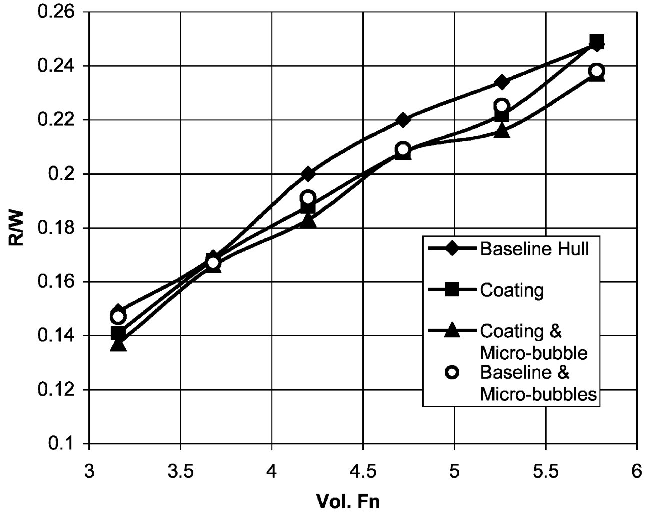

Fig. 5. Model catamaran resistance test results with/without MBDR system.

$$\Delta R_t = \left(\frac{R/W_{base} - R/W}{R/W_{base}}\right) \times 100\% \quad (1)$$

The percent change in resistance ΔR_t can be written in terms of the change from coating ΔR_c and micro-bubbles ΔR_b

$$\Delta R_t = \Delta R_c + \Delta R_b \quad (2)$$

When planning the model and ship tests with/without micro bubbles, we were aware that the drag reduction results would be in the range of 3–15% with an experimental uncertainty of 3–5% (standard deviation). The experimental uncertainty represents both variations in test speed as well as vibration contaminating the test data (Webster, 1992).

Subsequent filtering of the test data removed a significant part of model test vibrations and reduced the experimental uncertainty to 1.5–2.5%.

The test records and model photographs provided some insight into the affect of micro-bubbles and Coating A:

1. The micro-bubble system operation did not change model sinkage or trim.
2. The micro-bubble system operation did not change model air cavity pressure.
3. Consequently the wetted surface remained constant and therefore the micro-bubble system operation only reduced the drag of model.

The reduction in the coefficient of friction C_f with coating and micro-bubbles was determined using the following analysis. It allows comparison of the coating and micro-bubble covered areas against the baseline on the basis of local friction coefficient, C_f. This allows the resistance to be displayed as percent reduction of frictional resistance in terms of C_f/C_{fo}.

The following assumptions apply:

1. Brackish water with 16.5–17.6 ppt Salinity (Langly Towing Tank).
2. Water Temperature as in Table 3.
3. Uncoated surface C_{fo} estimated using ITTC model-ship correlation line given by

$$C_{fo} = \frac{0.075}{(\log_{10}R_N - 2)^2} \tag{3}$$

4. The catamaran is planing so the total resistance $R_T = R_P + R_f$ at constant speed, V = Constant.
5. There is no change in model trim or waterline in the model tests with/without coating.
6. The coated area $\beta = S_c/S_o$ is summarized in Table 3.
7. The value of

$$R_f = C_f \times \frac{1}{2}\rho V^2 S \tag{4}$$

8. Pressure resistance is unaffected by surface coating, $R_P = R_{Po}$.

This results in two expressions for no coating V = Constant (denoted by subscript "o")

$$R_{To} = R_{Po} + R_{fo} \tag{5}$$

and with Coating V = Constant

$$R_T = R_{Po} + (1-\beta)R_{fo} + \beta R_f \tag{6}$$

Subtracting Eq. (5) from Eq. (6) gives:

$$R_{To} - R_T = (R_{Po} - R_P) + R_{fo} - [(1-\beta)R_{fo} + \beta R_f] \tag{7}$$

Substituting Eq. (4) for R_f and R_{fo} and $\alpha = C_f/C_{fo}$ gives:

$$R_{To} - R_T = R_{Po} - R_p + C_{fo}S1/2\rho V^2 - C_{fo}S1/2\rho V^2(1-\beta)$$

$$+ \alpha\beta C_{fo}S1/2\rho V^2 \frac{R_{To} - R_T}{C_{fo}S1/2\rho V^2} = 1-(1-\beta)-\alpha\beta$$

$$\alpha\beta = \beta - \frac{R_{To} - R_T}{C_{fo}S1/2\rho V^2}$$

$$\alpha = C_f/C_{fo} = 1 - \frac{1}{\beta}\left(\frac{R_{To} - R_T}{C_{fo}S1/2\rho V^2}\right) \tag{8}$$

The value of α for coating A and MBDR were obtained from the resistance test

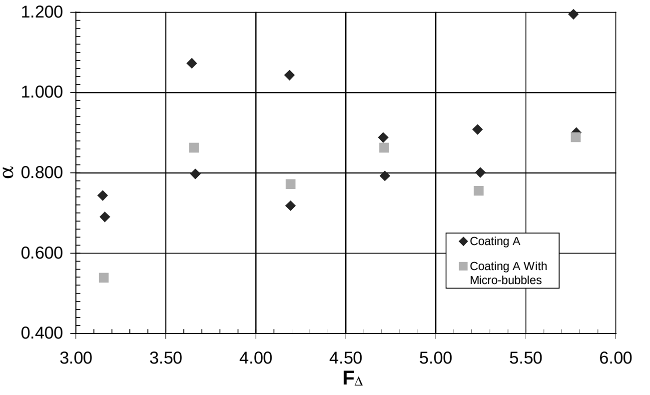

Fig. 6. Model localized drag reduction with coating and micro-bubbles.

data using Eq. (8). Fig. 6 shows the α value versus the displacement Froude number F_{∇}. The results show the decreases of α with test speed. To allow a more general interpretation of the test results, α is plotted as a function of Reynolds Number in Fig. 7.

5. Discussion and conclusions

Although coating the vessel hull sides with micro-bubbles occurs in most high-speed vessel applications, there is relatively little drag reduction data from tests with the micro-bubbles on vertical sides. Fortunately, Madavan et al. (1984) reported fresh water tunnel experiments on vertical plates. In these tests the tunnel velocity was

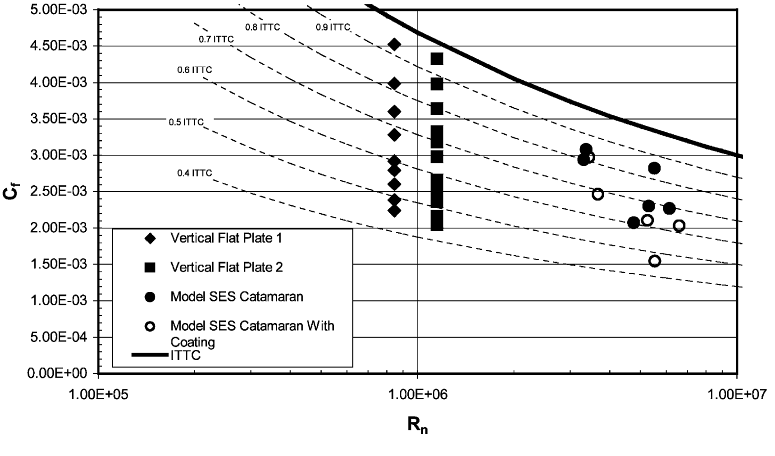

Fig. 7. Model catamaran resistance test results with/without MBDR system.

maintained constant (test 1 at $V = 9.3$ m/s, $Rn = 8.45 \times 10^5$ and test 2 at $V = 12.7$ m/s, $R_n = 1.15 \times 10^6$) and the gas flow rate changed to vary the value of C_v

$$C_v = \frac{Qa}{Qa + Qw} \tag{9}$$

where Q_a is the gas flow m^3/s. Q_w is the boundary layer flow m^3/s given by

$$Q_w = 0.9 \times \delta' \times h \times V \tag{10}$$

The turbulent boundary layer thickness δ is estimated at the trailing edge/vessel transom using an equivalent zero pressure-gradient, smooth flat plate with length $x = L$.

$$\delta = 0.373x^{4/5}(\nu/V)^{1/5} \tag{11}$$

The displacement thickness δ^* is estimated as:

$$\delta* = 0.125\delta \tag{12}$$

where $\delta' = (\delta - \delta*)$.

These results enable the estimation of the gas flow Q_a and the corresponding reduction in the local skin friction C_f/C_{fo} with and without non-wetting coating. The recommended design values are $Cv = 0.45$ to 0.5 giving the maximum reduction in local friction ($0.4 < C_f/C_{fo} < 0.85$) as shown in Fig. 8. These were used in the full-scale micro-bubble drag reduction system design.(Latorre et al., 2002b).

The results in Fig. 8 show an interesting result. The vertical flat plate data (Madavan et al., 1984) were recorded at constant velocity with variation in the air flow. In the model catamaran test, opposite conditions occurred with the test speed variable and the gas flow nearly constant. Consequently, at lower test speeds, the value of C_v was higher. At the lower speed the gas injection was large enough that only a portion of the micro-bubbles are effectively swept into the boundary layer.

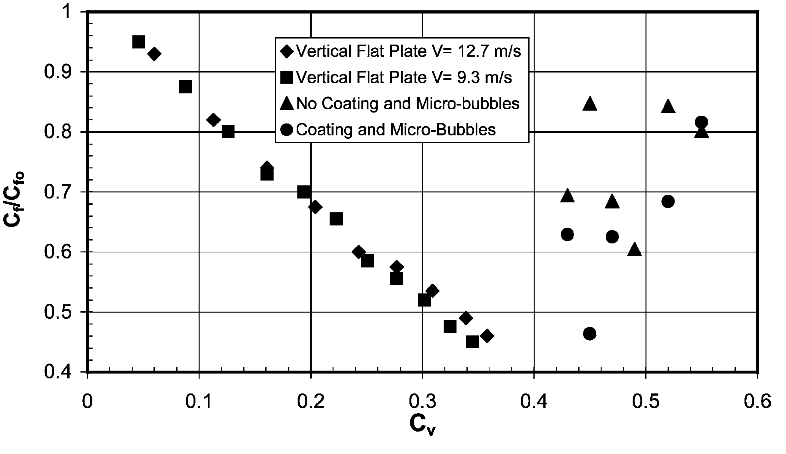

Fig. 8. Frictional drag reduction with vertical sides and microbubbles.

As the speed increases more gas enters into the boundary layer, resulting in an increase in drag reduction C_f/C_{fo}.

In conclusion, the 2.3 m SES catamaran micro-bubble drag reduction tests indicate the following:

1. The results of the micro-bubble injection on the vertical side of the 2.3 m SES catamaran showed drag reduction in the order of 5–8% with no coating and 8–11% with coating.
2. The results for the micro-bubble drag reduction on the vertical sides of the SES catamaran model achieved comparable levels of drag reduction as earlier flat plate tests.
3. The tests showed the drag reduction has greater sensitivity to the ratio of gas flow to the boundary layer flow C_v. The highest levels of micro-bubble drag reduction occur at rates of $0.4 < C_v < 0.5$.

Acknowledgements

The authors would like to thank the Gulf Coast Region Maritime Technology Center (GCRMTC), Dr. John M. Crisp, Executive Director, for their support. This project was completed under the Manufacturing Technology Program of the Office of Naval Research. The contents of this paper reflect the views of the authors, who are responsible for the facts and accuracy of the data presented herein. The contents do not necessarily reflect the official views or policies of the GCRMTC or its sites, the States of Louisiana or Texas, and the US Navy, or appropriate funding agency. This paper does not constitute a standard, specification, or regulation. The GCRMTC does not endorse products, equipment, or manufacturers. Trademarks or manufacturer names appear herein only because they are considered essential to the object of this report.

Appendix A

We performed the statistical Page Test (1954) on the resistance data records. This is often used in acoustic signal processing to resolve changes in the acoustic signals as to whether there is a real difference. The Page Test results are shown in Fig. 9 for model SES Catamaran resistance data record without and with micro bubbles. A zero value indicates no differences, as is the case with no micro-bubbles, and a large value shows the change with the micro-bubbles.

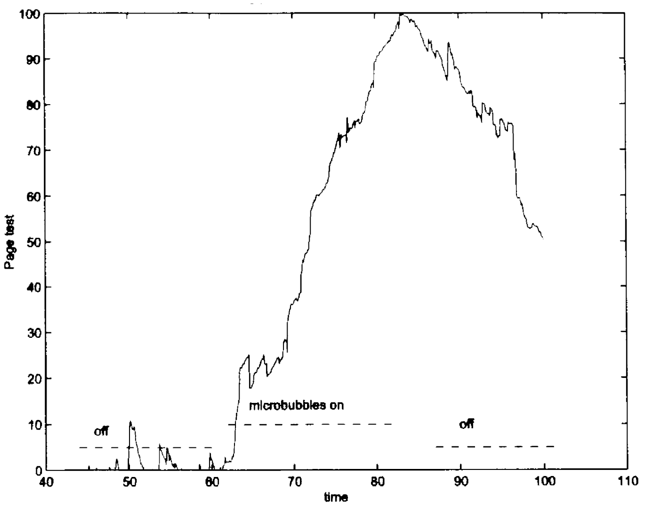

Fig. 9. Page's test results at displacement Froude number = 3.7, $V = 6.7$ m/s.

References

Fukuda, K., Tokunaga, J., Nobunaga, T., Nakatani, T., Iwasaki, T., Kunitake, Y., 2000. Frictional drag reduction with air lubricant over a super-water repellant surface. Journal of Marine Science and Technology 5, 123–130.

Kato, H., Iwashina, T., Miyanaga, M., Yamaguchi, H., 1999. Effect of microbubbles on the structure of turbulence in a turbulent boundary layer. Journal of Marine Science and Technology 4, 155–162.

Latorre, R., 1993. Enhancement of catamaran speed with bottom air flim. Proc. SNAME 5th Biennial Power Boat Symposium, Miami, FL, L1–L11.

Latorre, R., 1997. Ship hull drag reduction using bottom air injection. Ocean Engineering 24, 161–175.

Latorre, R., Bablenko, V., 1998. Role of bubble injection technique in drag reduction. Proc. ONR-NUWC International Symposium on Seawater Drag Reduction, Newport, RI, pp. 319–326.

Latorre, R., Miller, A., Philips, R., 2002a. Drag reduction with non-wetting and silcone coatings. Journal Naval Engineers (in press).

Latorre, R., Miller, A., Phillips, R., 2002b. Micro-bubble drag reduction for high speed craft. Trans. SNAME 110, pp. 259–277.

Madavan, N.K., Deutsch, S., Merkle, C.L., 1984. Reduction of turbulent skin friction by micro-bubbles. Physics of Fluids 27, 356–363.

Madavan, N.K., Deutsch, S., Merkle, C.L., 1985. Measurements of local skin friction in a microbubble-modified turbulent boundary layer. Journal of Fluid Mechanics 156, 237–256.

McCormick, M., Bhattacharyya, R., 1973. Drag reduction of a submersible hull by electrolysis. Naval Engineers Journal April, 11–16.

Merkle, C., Deutsch, S., 1992. Microbubble drag reduction in liquid turbulent boundary layers. Applied Mechanics Review 45, 103–127.

Page, E.S., 1954. Continuous inspection schemes. Biometrika 41, 100–115.

Phillips, R., Henoch, C., Latorre, R., Nuttal, G., 2001. Microbubble drag reduction on a surface effect ship model test at Langley Sea water Tow Tank. Proc. 26th ATTC, NY, paper 20.11.

Webster, W. (Ed.), 1992. Validation example—uncertainity analysis of a HSMV resistance test. Proc. 20th ITTC, Vol. 1, San Francisco, Sept. 1993, pp. 394–402.

Yun, L., Bliault, A., 1999. Theory and Design of Air Cushion Craft. John Wiley and Sons, New York, pp. 342–352.